5852 *Biochemistry* **2010,** *49,* 5852–5858
DOI: 10.1021/bi100566r

BIOCHEMISTRY
including biophysical chemistry & molecular biology
Article

Temperature Dependence of the Lumirhodopsin I−Lumirhodopsin II Equilibrium[†]

Istvan Szundi, Jacqueline Epps, James W. Lewis, and David S. Kliger*

Department of Chemistry and Biochemistry, University of California, Santa Cruz, California 95064

Received April 13, 2010; Revised Manuscript Received June 9, 2010

ABSTRACT: Time-resolved absorbance measurements, over a spectral range from 300 to 700 nm, were made at delays from 1 μs to 2 ms after photoexcitation of bovine rhodopsin in hypotonically washed membrane suspensions over a range of temperature from 10 to 35 °C. The purpose was to better understand the reversibility of the Lumi I−Lumi II process that immediately precedes Schiff base deprotonation in the activation of rhodopsin under physiological conditions. To prevent artifacts due to rotation of rhodopsin and its photoproducts in the membrane, probe light in the time-resolved absorbance studies was polarized at the magic angle (54.7°) relative to the excitation laser polarization axis. The difference spectrum associated with the Lumi I to Lumi II reaction was found to have larger amplitude at 10 °C compared to higher temperatures, suggesting that a significant back-reaction exists for this process and that an equilibrated mixture forms. The equilibrium favors Lumi I entropically, and van't Hoff plot curvature shows the reaction enthalpy depends on temperature. The results suggest that Lumi II changes its interaction with the membrane in a temperature-dependent way, possibly binding a membrane lipid more strongly at lower temperatures (compared to its precursor). To elucidate the origin of the time-resolved absorbance changes, linear dichroism measurements were also made at 20 °C. The time constant for protein rotation in the membrane was found to be identical to the time constant for the Lumi I−Lumi II process, which is consistent with a common microscopic origin. We conclude that Lumi II (the last protonated Schiff base photointermediate under physiological conditions) is the first photointermediate whose properties depend on the protein−lipid environment.

Considerable progress has been made during the past decade, since publication of the first 3-D crystal structure of rhodopsin (*1*), toward understanding the visual pigment activation mechanism and, more generally, that of G protein-coupled receptors (GPCRs).[1] Beginning with simple photoisomerization of the 11-*cis*-*N*-retinylidene chromophore, rhodopsin activation threads through multiple substructures and protonation "switches" at diverse locations within the transmembrane region of the protein (*2*−*4*). Beyond those diverse motifs internal to the protein, it has long been known that rhodopsin's lipid environment powerfully affects the later stages of activation. However, causal relationships between all of these parts and even the temporal sequence of their change have been difficult to establish, largely because experimental methods capable of resolving detailed structure require preparations stabilized using nonphysiological conditions. In order to better establish the sequence of events in visual pigment activation so that they can be understood *in vivo*, time-resolved measurements under physiological conditions are essential.

A primary advantage of time-resolved absorbance measurements reported here is their ability to characterize equilibria which have been shown to occur in several rhodopsin activation steps. To properly interpret results for thermally trapped species, the temperature dependence of these equilibria must be understood. The earliest reported thermal equilibrium in rhodopsin activation is the decay of bathorhodopsin (Batho) to form the blue-shifted intermediate (BSI) (*5*), a step immediately preceding formation of the lumirhodopsin (Lumi) photointermediate. Time-resolved absorbance characterization of the Batho ⇄ BSI equilibrium mixture provided the basis for more detailed characterization of the chromophore vibrations both in BSI and in the initially formed lumirhodopsin using resonance Raman spectral measurements (*6*). The strong temperature dependence of the Batho ⇄ BSI equilibrium was originally suggested to arise from ∼5 torsional modes of the *N*-retinylidene chromophore moving from above kT in Batho to below it in BSI (*7*), a molecular picture that could explain the otherwise puzzling, recently reported similarity between the behavior of the 12-methyl and 12-fluoro artificial retinal pigments in temperature trapping studies (*8*). In contrast to later equilibria, the processes up to and including formation of the initial form of lumirhodopsin, Lumi I, are independent of the protein environment (as shown by their lack of kinetic sensitivity to detergent solubilization), which suggests that changes are confined to the chromophore pocket of the protein. Later processes are known to be strongly affected by detergent solubilization (*9*), including the equilibrium between the metarhodopsin (Meta) photointermediates following Lumi II decay.

It remains to be determined exactly when and how the protein environment begins to affect photointermediate properties. The onset of this effect is important, because by reciprocity the earliest photointermediate sensitivity to protein surroundings, i.e., when environment affects the chromophore, reports when change has propagated to the surface of the protein−lipid complex. Previous

[†]This research was supported by Research Grant EY00983 from the National Eye Institute of the National Institutes of Health.

*Corresponding author: phone, (831) 459-2106; fax, (831) 459-4161; e-mail, kliger@chemistry.ucsc.edu.

[1]Abbreviations: Batho, bathorhodopsin; BSI, blue-shifted intermediate; GPCR, G protein-coupled receptor; Lumi, lumirhodopsin; Meta, metarhodopsin; ROS, rod outer segments; SB, *N*-retinylidene Schiff base; TBS, Tris-buffered saline; USID, unidirectional sequential intermediate difference.

 Published on Web 06/14/2010

studies have suggested that Schiff base (SB) deprotonation is the earliest process affected by detergents (*9*−*11*). However, here we examine the process immediately preceding the formation of the first SB deprotonated metarhodopsin (Meta) photointermediates to determine whether it too shows evidence of sensitivity to protein environment, several orders of magnitude earlier in time than SB deprotonation.

MATERIALS AND METHODS

Preparation of Hypotonically Washed, Rhodopsin Membrane Suspensions. Bovine rod outer segements (ROS) were prepared and hypotonically washed using 1 mM EDTA solution as previously described (*11*). After the final wash, the pellet was resuspended in TBS buffer (10 mM Tris, 60 mM KCl, 30 mM NaCl, 2 mM $MgCl_2$, 0.1 mM EDTA, adjusted to pH 7) and frozen in aliquots for later experiments. On the day of an experiment an aliquot was thawed, pelleted (Sorvall SS-34 rotor, 12K rpm, 20 min), and resuspended in low salt Tris buffer (10 mM Tris, 2 mM $MgCl_2$, 0.1 mM EDTA, pH 7) at a final rhodopsin concentration of 1.1−1.5 mg/mL.

Time-Resolved Absorbance Measurements at Magic Angle. Time-resolved absorbance changes from 300 to 700 nm were measured at temperatures from 10 to 35 °C using an apparatus described previously (*12*). Absorbance difference spectra were collected at a series of delay times, ranging from 2 μs to 2 ms at 10 and 20 °C and from 500 ns to 64 μs at 35 °C, after the ∼7 ns excitation pulse of 477 nm light (80 μJ/mm^2). Polarization of the probe light was set to 54.7° (magic angle) relative to the excitation pulse polarization in order to prevent absorbance changes due to rotational diffusion of rhodopsin in the membrane from being recorded. Prior to performing measurements, to reduce light scattering, samples were sonicated for 30 s under argon in an ice bath.

Data Analysis Using Global Fitting. Each set of time-dependent absorption difference spectra (after averaging multiple experiments at each temperature and noise reduction using singular value decomposition), $\{\Delta A(\lambda,t)\}$, was fit to functions of the form:

$$\Delta a(\lambda,t) \equiv b_0(\lambda) + b_1(\lambda)e^{-t/\tau_1} + b_2(\lambda)e^{-t/\tau_2} + ...$$

with two, three, and four exponential terms (*5*). Global fitting gives the time constants, τ_i, for the exponential processes and the b-spectra, $b_i(\lambda)$, or difference spectra associated with those time constants. The number of exponentials that best fit the data was determined from plots of residuals, $\Delta A(\lambda,t) - \Delta a(\lambda,t)$. When the proper number of exponential terms are fit, residual plots should be flat and not significantly improved by an additional exponential term. Even if the evolution of photointermediates follows the simplest mechanism, i.e., Lumi I → Lumi II → Meta X, the b-spectra would not correspond exactly to the difference spectra between successive photointermediates; i.e., $b_1(\lambda)$ is not equal to $A_{\text{Lumi I}}(\lambda) - A_{\text{Lumi II}}(\lambda)$, because any sum of exponential function results from a model where all time-dependent spectral changes start at $t = 0$. Clearly, this is not true for the simple sequential model above because Meta X formation only begins at some delay after initial photolysis, specifically after Lumi II is formed. The actual difference spectra between successive photointermediates for the above simplest, unidirectional sequential model have to be constructed from linear combinations of the b-spectra (*13*). The amount of mixing between temporally adjacent b-spectra is approximately proportional to the ratio of their time constants. The difference spectra between successive photointermediates constructed in that manner are referred to here as unidirectional sequential intermediate difference (USID) spectra. A USID spectrum should be temperature independent, both in shape and in amplitude, if the associated reaction is actually unidirectional and the spectra of the successive photointermediates are temperature independent, an assumption commonly made for photointermediates (*14*).

Linear Dichroism Measurements. To characterize rotational diffusion of rhodopsin in membrane suspensions, time-resolved absorbance measurements were made at a series of time delays using probe light that was linearly polarized along an axis either parallel to, $\Delta A_{\parallel}(\lambda,t)$, or perpendicular to, $\Delta A_{\perp}(\lambda,t)$, the polarization axis of the excitation laser. Samples used here for linear dichroism measurements were not sonicated (although mild sonication does not appear to significantly affect the data). A number of experimental conditions were changed to improve dichroic ratios in the linear dichroism data. Depolarization of both probe and excitation light due to scattering was reduced by using lower rhodopsin concentration than was used for the polarization averaged, absorbance magic angle experiments described above (0.4−0.5 mg/mL rhodopsin versus 1.1−1.5 mg/mL for magic angle experiments). Flow in linear dichroism experiments was identical to that in magic angle measurements. Dichroic ratios were also improved by using lower excitation fluences (40 μJ/mm^2) than those described above for magic angle measurements. Finally, more collimated probe light was produced in the linear dichroism measurements by using an iris to restrict the aperture of the lens focusing probe light onto the sample. Measurements reported here were made using a cone of rays with 3°, half-angle. These steps improved the dichroic ratios somewhat from what was previously reported for Lumi I (*11*). The above measures all improved dichroic ratios obtained, but each significantly reduced the signal-to-noise ratio of the data compared to what could be obtained in the magic angle experiments.

RESULTS

Figure 1 shows averaged data from a series of time-resolved absorbance experiments conducted at 35 °C and magic angle polarization.

As can be deduced from the large gap between the difference spectra collected at delays of 32 and 64 μs after photoexcitation, substantial absorbance changes continued after the last time point shown, but in order to best resolve the relatively small Lumi II formation process, data collection was primarily focused at the times when it occurred. Enough data were collected here subsequent to Lumi II formation so that an exponential term could be fit to the slow processes immediately following Lumi II formation, accounting for their effects on the time scale we study. A similar procedure was previously applied to data for rhodopsin at 20 °C first in detergent (*15*) and then in membrane (*12*), allowing Lumi II formation to be characterized under those conditions. Even though data were collected at longer times for the lower temperatures studied here (up to 128 μs at 20 °C and 2 ms at 10 °C), the extent of progress was smaller at those temperatures than at 35 °C, which resulted in significantly more overlap of the plotted curves at those temperatures (data is not shown).

The averaged data we collected required three exponential terms for the best fit at all temperatures. Residuals from two and three exponential fits are compared in Figure 2 for the averaged

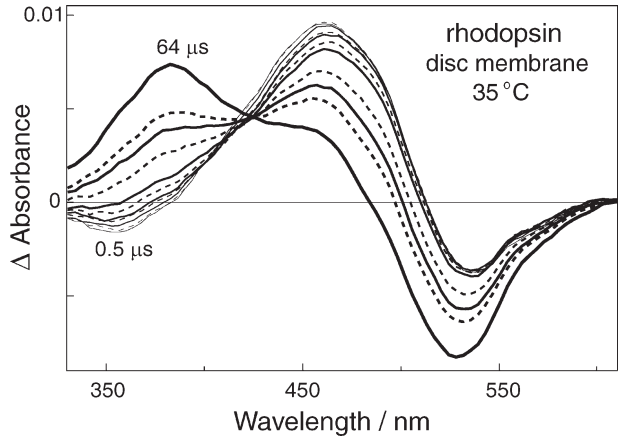

FIGURE 1: Absorbance difference spectra measured at a series of time delays after photoexcitation of bovine rhodopsin in its native disk membrane with a 7 ns pulse of 477 nm light at 35 °C. Progressively thicker lines (alternating solid and dashed) show the averaged data that were collected at time delays: 0.5, 1, 2, 3, 4, 6, 8, 16, 24, 32, and 64 μs. Significant absorbance changes take place after 64 μs, continuing the process seen above from 16 to 64 μs, but the primary goal of the current work is to characterize the relatively small amplitude process which takes place over the time range from 2 to 8 μs at this temperature.

data collected at 10, 20, and 35 °C. At every temperature, the shaded areas show that including a third exponential term in the fitting function improved the fit of several of the earliest absorbance difference spectra we recorded. The time constants determined from the three exponential fits are given in Table 1. As shown there, the fast lifetime was submicrosecond at 20 and 35 °C and only slightly longer than that at 10 °C, which suggests it arises from fitting the tail of the Lumi I formation process.

Agreement between the fast process lifetimes given in Table 1 and those previously determined for Lumi I formation (*5*) is reasonable given that data collection here only started after at least one lifetime of the fast process had elapsed. The b-spectra shapes determined for the fast process were also consistent with attribution of the fast process to an equilibrated mixture, i.e., bathorhodopsin (Batho) ⇄ blue-shifted intermediate (BSI), decaying to Lumi I. However, because the data collected here started after most of Lumi I was formed, the b-spectra coefficients of the fast exponential were not determined as precisely as in previously reported experiments specifically designed to characterize Lumi I formation. For clarity, Figure 3 shows only the well-determined b-spectra coefficients of the Lumi II formation exponential term and of the exponential term fit to the slower Lumi II decay processes at the three temperatures studied.

The Lumi I−Lumi II exponential term b-spectrum amplitude in Figure 3 is largest at 10 °C and becomes progressively smaller as the temperature is increased. We had to acquire and average substantial amounts of data to resolve the small component associated with Lumi I−Lumi II at 35 °C. The relative size of that component is even smaller than it appears from comparison of the curves in the top panel of Figure 3 since the late, very slow processes do not manifest themselves completely on the time scale we study, which results in an artificial attenuation of $b_0(\lambda)$. If followed to completion at 35 °C, the final peak to trough difference when Meta II completely forms would be ~0.08. The higher signal-to-noise ratio measurements made here to resolve this small component in the presence of such large changes probably accounts for the fact that the even smaller changes associated with Lumi I formation at 20 °C were noticed here but not in earlier studies (*12*).

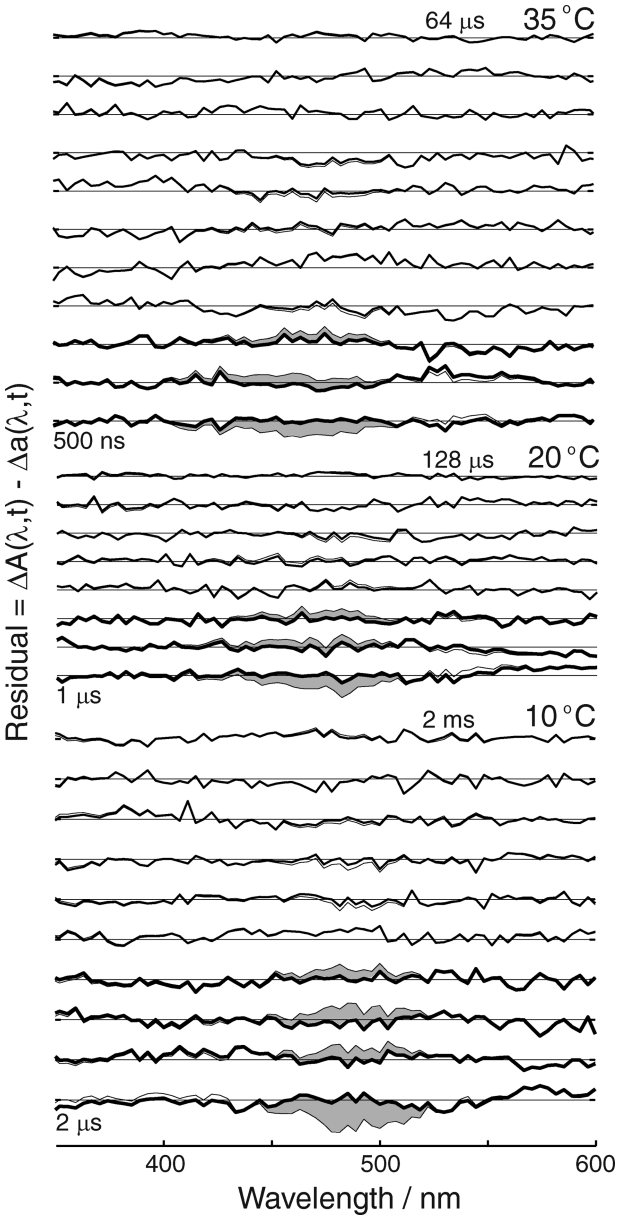

FIGURE 2: Residual plots for two and three exponential fits of the absorbance difference data. Thin lines show the residuals, $\Delta A(\lambda,t) - \Delta a(\lambda,t)$, for fits to the data at each temperature using two exponential terms, and thicker lines show the residuals for the three exponential fits. The thickest lines (at the early delay times) show where the greatest improvement in residuals was obtained from using three exponential terms. Residuals were offset in these plots by 0.001 (10 °C) and 0.0005 (20 and 35 °C) as shown by the straight zero lines. Areas where the most significant improvement in residuals was achieved by the three exponential fits are highlighted in gray.

Table 1: Exponential Lifetimes from Global Fitting

temp (°C)	τ_{fast} (μs)	$\tau_{Lumi\ II\ formation}$ (μs)	τ_{slow} (μs)
10	1.6 ± 0.5	31 ± 2	2700 ± 200
20	0.50 ± 0.3	10 ± 1	82 ± 5
35	0.21 ± 0.05	2.8 ± 0.3	43 ± 5

The steady decrease in amplitude of the spectral change associated with the Lumi I−Lumi II process with temperature strongly suggests that a more complex reaction is taking place than a simple unidirectional conversion of one intermediate into another. However, a b-spectrum only approximates the spectral change between a

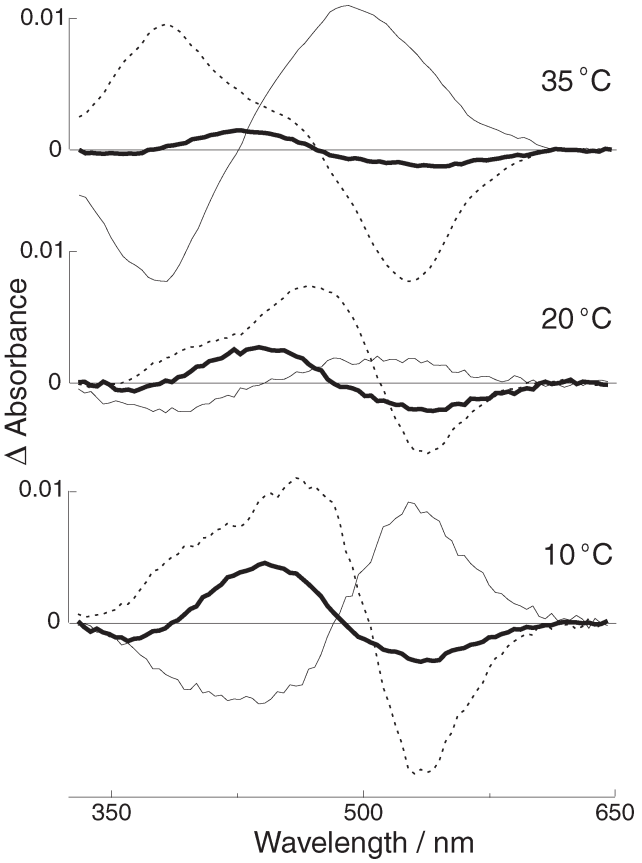

FIGURE 3: Difference spectra from the global exponential fit associated with the Lumi I−Lumi II process and extrapolated slower processes at each measurement temperature. Heavy lines show the b-spectrum coefficient of the Lumi I−Lumi II exponential term at each temperature. Light lines show the single b-spectrum fit to each temperature's data that accounts for the processes taking place after the Lumi I−Lumi II process is complete. Dotted lines show each temperature's constant term, $b_0(\lambda)$, which is the extrapolated difference spectrum after all exponential terms have decayed to zero. Note that only a few time points were collected here after the Lumi I−Lumi II process was complete, which allows subsequent events to be accounted for by a single exponential term. However, for the same reason the slower processes did not proceed very far; neither the slow process b-spectrum nor $b_0(\lambda)$ accurately represents what happens when measurements are made at much later times than were studied here (see, for example, Thorgeirsson et al. (*16*)).

pair of sequential intermediates, and any firm conclusion must be based on the unidirectional sequential intermediate difference spectrum.

To determine whether the Lumi I−Lumi II process follows a unidirectional sequential scheme, USID spectra were calculated using the observed lifetimes and b-spectra at the three temperatures studied. Figure 4 shows a plot of the results (after normalizing the Lumi I−Lumi II USID amplitudes so that their shapes can be compared).

The similarity of the USID shapes at all temperatures suggests that the process involves two intermediates with temperature-independent spectra, but the fact that the amplitude of the USID spectrum decreases with temperature (when not normalized as was done in Figure 4, the USID amplitude decreases by a factor of 1.6 in going from 10 to 20 °C and by a factor of 2.6 between 10 and 35 °C) suggests that the reaction between Lumi I and Lumi II is not unidirectional and that the correct scheme instead includes a back-reaction that becomes more significant as the temperature increases. The data give clear evidence that the resulting

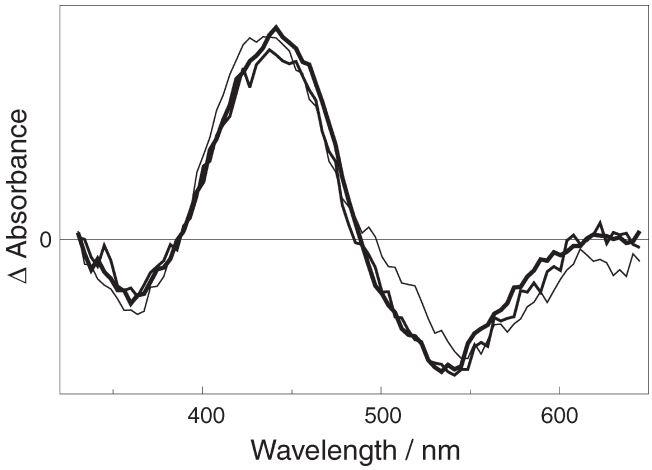

FIGURE 4: Normalized difference spectra of the Lumi I−Lumi II process after correction for mixing with the slow process b-spectrum. The sum of exponentials fit to the data produces b-spectra of processes that all begin at the same zero of time. This amounts to assuming that the slow process occurs in parallel with the fast process. Since the slow process can only start after the earlier processes finish, the slow process b-spectrum erroneously includes changes that actually belong to the difference spectrum of its preceding process. The effect becomes larger as the two processes' time constants become closer. A linear combination of b-spectra must be used to construct unidirectional sequential intermediate difference spectra which describe a unidirectional reaction scheme. The heavy line shows the corrected USID spectrum of the Lumi I−Lumi II process seen at 10 °C with thinner lines showing the corrected difference spectrum at 20 and 35 °C after scaling for comparison. The 20 °C difference spectrum was scaled by a factor of 1.5, and the 35 °C difference spectrum was scaled by 2.6.

Table 2: Lumi I ⇄ Lumi II Equilibrium Constant versus Temperature

absolute temp (K)	f	$K_{\text{Lumi I} \rightleftarrows \text{Lumi II}}$
283	0.8 ± 0.01	4.0 ± 0.25
293	0.53 ± 0.015	1.1 ± 0.07
308	0.3 ± 0.02	0.44 ± 0.04

equilibrium constant, $K_{\text{Lumi I} \rightleftarrows \text{Lumi II}}$, decreases with temperature, but the values of the equilibrium constant as a function of temperature cannot be directly determined from the difference spectra alone. At any particular temperature, a range of equilibrium constant values could produce the observed difference spectrum, depending on the spectral characteristics of Lumi I and Lumi II. However, the spectral shapes of known rhodopsin photointermediates do not vary widely, and their properties can be used to constrain estimates of f, the fraction of Lumi I converted to Lumi II at equilibrium. To estimate f, we calculated the spectrum of Lumi II for a range of candidate f values in terms of the Lumi I spectrum using the relation:

$$\text{Lumi II}(\lambda) = \text{Lumi I}(\lambda) + [\text{USID}_{\text{Lumi I} \rightleftarrows \text{Lumi II}(\lambda)} / f]$$

The result was that for f less than 0.8 at 10 °C, the spectrum of Lumi II required to fit the data became narrower than the known spectra of rhodopsin and Lumi I, suggesting that for a Lumi II with similar spectral properties to rhodopsin and Lumi I, $f = 0.8$ at 10 °C. Using this value, the equilibrium constants given in Table 2 were calculated from the data.

Modeling suggests the intermediate spectra have λ_{max} values of 488 nm for Lumi I and 496 nm for Lumi II, with similar extinction coefficients for the photointermediates.

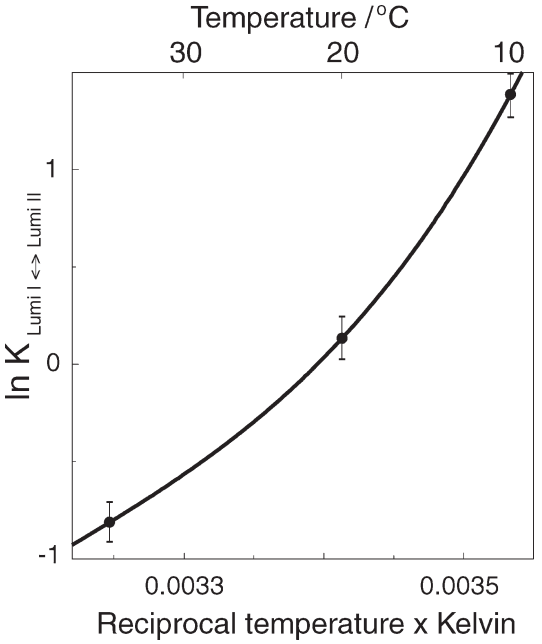

FIGURE 5: van't Hoff plot for Lumi I ⇄ Lumi II equilibrium. Points show the natural logarithm of the K_{eq} determined for the Lumi I ⇄ Lumi II equilibrium versus the reciprocal of the absolute temperature. Error bars are plotted at the level that would be produced by uncertainty in the amplitude of the USID spectra propagated into K_{eq} values. The data are best fit by a curved line suggesting that the slope (the negative enthalpy of the Lumi I ⇄ Lumi II process divided by R, the gas constant), and hence the ΔH of reaction, changes with temperature.

A van't Hoff plot of $\ln(K_{\text{Lumi I} \rightleftarrows \text{Lumi II}})$ versus the reciprocal of the absolute temperature is shown in Figure 5.

Where such a plot is linear, the slope gives the negative enthalpy change for the Lumi I ⇄ Lumi II reaction divided by the gas constant, R. The points in our van't Hoff plot do not follow a straight line, and the deviation from linearity is outside the uncertainty in the $K_{\text{Lumi I} \rightleftarrows \text{Lumi II}}$ values. The fact that a curved line best fits the data suggests that the reaction enthalpy depends on temperature. The intercept of the van't Hoff plot gives the reaction entropy, which is clearly negative.

Figure 6 shows linear dichroism data collected on a time scale similar to that of the magic angle time-resolved absorbance data. The best single exponential fit to the decay of linear dichroism at 20 °C had a time constant of 24 μs. A somewhat better fit was obtained using two exponential terms with lifetimes of 12 and 48 μs, which is consistent with the theory of linear dichroism relaxation due to protein rotation in randomly oriented lipid bilayers (*17*). The fact that a residual component of the linear dichroism does not relax on this time scale, even when rotational diffusion within the membrane is complete, is also predicted by that theory.

DISCUSSION

Our time-resolved UV/visible absorbance measurements complement information obtained by other techniques which provide more structural information but less temporal resolution. Solid-state NMR, FTIR, and X-ray crystalography have all been very useful for characterizing temperature and/or pH-trapped forms of rhodopsin photointermediates (*2*, *18*, *19*), but ultimately all studies of trapped intermediates need to be carefully correlated with the unconstrained physiological process. In particular, kinetic studies are useful to detect and characterize metastable

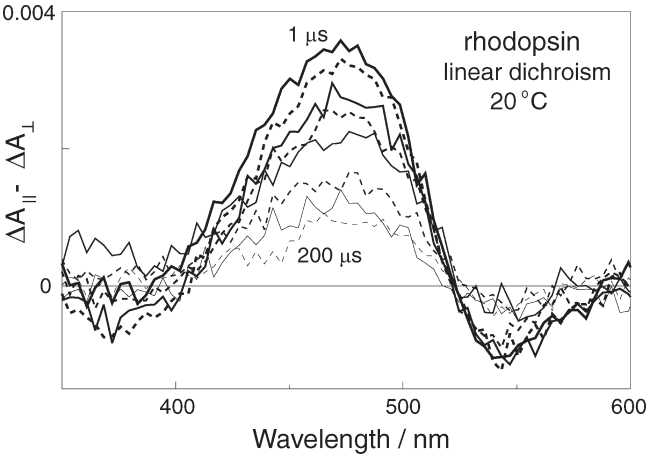

FIGURE 6: Linear dichroism observed after photoexcitation of bovine rhodopsin in its native disk membrane with a 7 ns pulse of 477 nm light at 20 °C. Progressively thinner lines (alternating solid and dashed) show the averaged data that were collected at time delays: 1, 2, 5, 10, 20, 50, 100, and 200 μs. For this sample, $(\Delta A_{\parallel} + 2\Delta A_{\perp})/3$ (which corresponds to the absorbance change measured at magic angle polarization) had a maximum value of 0.004 near 470 nm.

equilibrium mixtures whose properties may be fundamental to understanding trapped photointermediates. Further, even the highest resolution studies of the currently known, trapped photointermediate forms leave large gaps in the sequence of activation pictures. Even though details may be sparse, kinetic optical studies fill in the gaps between those pictures. At the very least, time-resolved absorbance studies define the intermediate forms that need to be trapped and time domains where more structurally rich methods need to be applied. However, in favorable cases the absorbance spectra of photointermediates and the time constants of optical processes can themselves give information about the underlying process.

The largest absorbance changes that occur after rhodopsin photoexcitation are caused by deprotonation of the *N*-retinylidene Schiff base (SB) to form products absorbing near 380 nm. SB deprotonation is an important marker, because a rhodopsin photoproduct with a deprotonated SB is the usual activator of transducin, rhodopsin's G protein (*2*). NMR measurements have reported significant translation of the chromophore relative to the protein after SB deprotonation, including an ~5 Å shift in the *N*-retinylidine β-ionone ring toward helix 5 (*18*). However, little is known about when and how this translation occurs, and the preceding steps we study are clearly critical to an understanding of rhodopsin's activation process. Near physiological temperatures Lumi II is the last protonated SB photointermediate, as demonstrated by the direct production of 380 nm absorbance in the b-spectrum of the slow, Lumi II decay process forming Meta I_{380}, shown at 35 °C in Figure 3. Thus, although the spectral shift in the Lumi I−Lumi II process may be small, the process appears to be significant for understanding SB deprotonation and the broader sequence of molecular changes leading to the G protein activating form.

Lumi I−Lumi II Is an Equilibrium Process in Membrane. Recognition of the Lumi I−Lumi II process was impeded at 20 °C by the similarity of the Lumi I−Lumi II time constant to the time constant for protein rotational diffusion in the native disk membrane. Originally, Lumi I−Lumi II studies concentrated on resolving the process in detergent suspensions (where molecular rotation effects on the Lumi I−Lumi II time scale are

absent) and characterizing the process in membrane samples at 20 °C (*12*, *15*). The current temperature study of the Lumi I−Lumi II process in membrane was undertaken in order to determine whether the Lumi I−Lumi II reaction is unidirectional or involves an equilibrium mixture, as is the case for several other rhodopsin photointermediate reactions. Some of these equilibrium processes (such as the Batho−BSI process) have been shown to be independent of whether rhodopsin's environment is membrane or detergent (*11*), while others (such as the Meta I_{480}−Meta II process) depend strongly, both in equilibrium constant and in rate, on whether membrane or detergent preparations are studied (*9*, *10*). Prior to the current work, it had not been established whether Lumi I−Lumi II was an equilibrium process. Further, the effects of detergent solubilization on its rate and difference spectrum seemed to lie between the two extremes of behavior. While the original 20 °C study comparing membrane and detergent behavior showed that the rate of the Lumi I−Lumi II process was independent of detergent solubilization, the difference spectra associated with the process in membrane and in detergent were not identical (*12*), suggesting that detergent affected the spectrum of Lumi II but not the rate of the Lumi I−Lumi II process, a characteristic which may be a clue to understanding the molecular basis of the change involved.

The fact that the difference spectrum of the Lumi I−Lumi II process at 35 °C, shown in Figure 4, is similar in shape to, but has only ~40% of the amplitude of, the 10 °C difference spectrum strongly suggests that a temperature-dependent equilibrated mixture of the two photointermediates occurs in membrane, with the equilibrium being more forward shifted at lower temperature (i.e., Lumi I favored entropically). This behavior was not shared by results obtained after photoexcitation of detergent-solubilized rhodopsin samples where little or no increase in the amplitude of the Lumi I−Lumi II difference spectrum was seen at 10 °C compared to 35 °C (*20*). It is probably significant that detergent affects the Lumi I−Lumi II equilibrium constant at low temperatures. This demonstrates that the Lumi I−Lumi II reaction is the earliest process where the state of the protein−lipid interface begins to affect kinetic rates. That observation suggests the need for caution in the interpretation of experiments at lower temperatures on later rhodopsin photointermediates, which are likely to be strongly perturbed by artificial experimental conditions. Of more positive significance for the physiological activation mechanism, in contrast to the weak effect on rates, detergent strongly affects the difference spectrum computed for the Lumi I−Lumi II process, suggesting that Lumi II is the first photointermediate where the lipid environment affects the chromophore. Thus, while the Lumi II formation rate is not markedly detergent dependent over the temperature range studied here, its subsequent reactions, both forward and back, show significant detergent dependence. Further, since the equilibrium between Lumi I and Lumi II forward shifts as the temperature is lowered, Lumi II must be the classical form of lumirhodopsin that is temperature trapped. Presumably the situation is analogous for the Lumi photointermediate of cone visual pigments if a similar Lumi I−Lumi II transition exists there. The limited availability and stability of cone pigments continue to confine photointermediate characterization to low temperature methods which do not detect a Lumi I−Lumi II transition (*21*).

Lumi I ⇄ Lumi II Is Exothermic in Membrane. The positive slope of the van't Hoff plot for the Lumi I ⇄ Lumi II equilibrium in Figure 5 indicates that the enthalpy change, ΔH, for the reaction is negative. As discussed above this appears not to be the case for detergent-solubilized samples. This observation is consistent with a picture where Lumi I and Lumi II differ in their interactions with the membrane lipid environment, with Lumi II interacting more strongly, releasing heat when Lumi II is formed. One way this could arise in membrane is for Lumi II to manifest some change at the protein−lipid interface such that the protein associates more strongly with one or more membrane lipids. The strength of this interaction could depend on membrane bilayer properties such as an order bias along the transmembrane helical orientation or solubility of lipid components in the membrane. The lack of comparable phenomena in micelles could eliminate the exothermicity in detergent preparations accounting for absence of slope in the comparable plot for detergent-solubilized rhodopsin (not shown). Electron crystallography of two-dimensional crystals of rhodopsin at liquid nitrogen temperatures has revealed density assigned to a bound cholesterol molecule which may change its interaction with the protein in the Lumi I−Lumi II transition in the native membrane environment near room temperature (*22*). Partial immobilization of one or more lipids in the Lumi I−Lumi II process would also be a mechanism to account for the negative entropy change (deduced from the negative intercept likely in the van't Hoff plot) associated with the equilibrium.

The upward curvature of the van't Hoff plot for the Lumi I−Lumi II process in membrane indicates that the ΔH becomes more negative at lower temperatures, favoring Lumi II. Such a strong temperature dependence of the equilibrium constant is unusual and may indicate molecular processes beyond those considered above. Rhodopsin dimers have been observed in two-dimensional crystals of rhodopsin (*22*), and a temperature- and/or photointermediate-dependent change in the association constant for dimer formation in membrane could account for the observed temperature-dependent ΔH. Time-resolved linear dichroism studies of photoselected rhodopsin suggest higher order aggregates are not present to any significant degree in the bovine disk membrane at 20 °C, but their contribution at lower temperatures cannot be excluded. Alternatively, membrane bilayer bulk properties which affect solubility of membrane components are certainly temperature dependent, so there are a number of possible explanations for the temperature-dependent strength of interaction reflected in ΔH.

Rotational Diffusion and Lumi I−Lumi II Equilibration Have Similar Time Scales. The linear dichroism data in Figure 6 show that the time constant for rotational diffusion of rhodopsin and its photoproducts within the membrane bilayer is identical to the time constant of Lumi I−Lumi II equilibration at 20 °C. The major component of the linear dichroism shown in Figure 6 relaxes with a time constant of 12 μs, essentially identical to the 10 μs time constant given in Table 1 for the Lumi I−Lumi II process at that temperature. The coincidence of the time scales of these two phenomena raises the possibility that the Lumi I−Lumi II process is in some way coupled to thermal motion of rhodopsin within the membrane. Although the simplest models of rotational diffusion consider the rotating molecule to be a rigid body, for a heptahelical transmembrane protein such models are obviously only an approximation, and thermal motion of individual helices or other substructures (such as the H5−H7 and H2−H4 substructures proposed by Chelikani et al. (*23*)) presumably takes place on a similar time scale as rotation of the aggregate body. Substructure motion due to membrane lipid fluctuations could facilitate reorganization of the hydrogen-bonded network which has been implicated in rhodopsin activation (*24*, *25*). Prior to

chromophore photoisomerization, the network of hydrogen bonds within the protein is expected to have a relatively definite state as compared to the state which must exist in the early photointermediates, where the dark, hydrogen-bonded state has been disrupted and not yet replaced by another relatively ordered state, which presumably catalyzes receptor activation. The entropy decrease we report here in the Lumi I−Lumi II process may be due to the restoration of a more ordered internal hydrogen-bonded network in a reorganized configuration that facilitates receptor activation. That hypothesis is supported by the observation of significant reductions in PSB stability at the Lumi II stage in rhodopsin mutants S186A and E181F which potentially disrupt reorganization of the hydrogen-bonded network in the vicinity of the chromophore (*24*, *26*). Reorganization of the chromophore and/or the hydrogen-bonded network in its vicinity during the Lumi I−Lumi II process or shortly thereafter is also suggested by time-resolved circular dichroism changes that take place on that time scale (*27*).

Although better characterization of the structural features that distinguish Lumi I from Lumi II is needed, there is no doubt that this change has critical physiological significance for the mechanism of G protein-coupled receptor activation. G proteins can only be activated when GPCRs change their surface properties. Thus we stress that the current measurements characterize the earliest photointermediate of rhodopsin whose properties depend on conditions at the lipid−protein interface. Further, the Lumi II photointermediate characterized here forms under physiological conditions rather than in artificial circumstances, giving it unquestionable standing as the threshold of Schiff base deprotonation and transducin activation.

REFERENCES

1. Palczewski, K., Kumasaka, T., Hori, T., Behnke, C. A., Motoshima, H., Fox, B. A., Le Trong, I., Teller, D. C., Okada, T., Stenkamp, R. E., Yamamoto, M., and Miyano, M. (2000) Crystal structure of rhodopsin: a G protein-coupled receptor. *Science 289*, 739–745.
2. Hofmann, K. P., Scheerer, P., Hildebrand, P. W., Choe, H.-W., Park, J. H., Heck, M., and Ernst, O. P. (2009) A G protein-coupled receptor at work: the rhodopsin model. *Trends Biochem. Sci. 34*, 540–552.
3. Mahalingam, M., Martínez-Mayorga, K., Brown, M. F., and Vogel, R. (2008) Two protonation switches control rhodopsin activation in membranes. *Proc. Natl. Acad. Sci. U.S.A. 105*, 17795–17800.
4. Birge, R. R., and Knox, B. E. (2003) Perspectives on the counterion switch-induced photoactivation of the G protein-coupled receptor rhodopsin. *Proc. Natl. Acad. Sci. U.S.A. 100*, 9105–9107.
5. Hug, S. J., Lewis, J. W., Einterz, C. M., Thorgeirsson, T. E., and Kliger, D. S. (1990) Nanosecond photolysis of rhodopsin: evidence for a new, blue-shifted intermediate? *Biochemistry 29*, 1475–1485.
6. Pan, D. H., Ganim, Z., Kim, J. E., Verhoeven, M. A., Lugtenburg, J., and Mathies, R. A. (2002) Time-resolved resonance Raman analysis of chromophore structural changes in the formation and decay of rhodopsin's BSI intermediate. *J. Am. Chem. Soc. 124*, 4857–4864.
7. Lewis, J. W., and Kliger, D. S. (1992) Photointermediates of visual pigments. *J. Bioenerg. Biomembr. 24*, 201–210.
8. Bovee-Geurts, P. H. M., F., Fernández, I. F., Liu, R. S. H., Mathies, R. A., Lugtenburg, J., and DeGrip, W. J. (2009) Fluoro derivatives of retinal illuminate the decisive role of the C_{12}-H element in photoisomerization and rhodopsin activation. *J. Am. Chem. Soc. 131*, 17933–17942.
9. Baker, B. N., Donovan, W. J., and Williams, T. P. (1977) Extractant effects on some properties of rhodopsin. *Vision Res. 17*, 1157–1162.
10. Applebury, M. L., Zuckerman, D. M., Lamola., A. A., and Jovin, T. M. (1974) Rhodopsin. Purification and recombination with phospholipids assayed by the metarhodopsin I → metarhodopsin II transition. *Biochemistry 13*, 3449–3458.
11. Lewis, J. W., Einterz, C. M., Hug, S. J., and Kliger, D. S. (1989) Transition dipole orientations in the early photolysis intermediates of rhodopsin. *Biophys. J. 56*, 1101–1111.
12. Epps, J., Lewis, J. W., Szundi, I., and Kliger, D. S. (2006) Lumi I → Lumi II: the last detergent independent process in rhodopsin photoexcitation. *Photochem. Photobiol. 82*, 1436–1441.
13. Szundi, I., Lewis, J. W., and Kliger, D. S. (1997) Deriving reaction mechanisms from kinetic spectroscopy. Application to late rhodopsin intermediates. *Biophys. J. 73*, 688–702.
14. Nagle, J. F. (1991) Solving complex photocycle kinetics. Theory and direct method. *Biophys. J. 59*, 476–487.
15. Szundi, I., Lewis, J. W., and Kliger, D. S. (2003) Two intermediates appear on the lumirhodopsin time scale after rhodopsin photoexcitation. *Biochemistry 42*, 5091–5098.
16. Thorgeirsson, T. E., Lewis, J. W., Wallace-Williams, S. E., and Kliger, D. S. (1993) Effects of temperature on rhodopsin photointermediates from lumirhodopsin to metarhodopsin-II. *Biochemistry 32*, 13861–13872.
17. Cherry, R. J., and Godfrey, R. E. (1981) Anisotropic rotation of bacteriorhodopsin in lipid-membranes—comparison of theory with experiment. *Biophys. J. 36*, 257–276.
18. Patel, A. B., Crocker, E., Eilers, M., Hirshfeld, A., Sheves, M., and Smith, S. O. (2004) Coupling of retinal isomerization to the activation of rhodopsin. *Proc. Natl. Acad. Sci. U.S.A. 101*, 10048–10053.
19. Nakamichi, H., and Okada, T. (2006) Crystallographic analysis of primary visual photochemistry. *Angew. Chem., Int. Ed. 45*, 4270–4273.
20. Epps, J. J. (2008) Effects of different environments on rhodopsin photochemistry, Dissertation, University of California at Santa Cruz, Santa Cruz, CA.
21. Kusnetzow, A., Dukkipati, A., Babu, K. R., Singh, D., Vought, B. W., Knox, B. E., and Birge, R. R. (2001) The photobleaching sequence of a short-wavelength visual pigment. *Biochemistry 40*, 7832–7844.
22. Ruprecht, J. J., Mielke, T., Vogel, R., Villa, C., and Schertler, G. F. X. (2004) Electron crystallography reveals the structure of metarhodopsin I. *EMBO J. 23*, 3609–3620.
23. Chelikani, P., Hornak, V., Eilers, M., Reeves, P. J., Smith, S. O., RajBhandary, U. L., and Khorana, H. G. (2007) Role of group-conserved residues in the helical core of β_2-adrenergic receptor. *Proc. Natl. Acad. Sci. U.S.A. 104*, 7027–7032.
24. Yan, E. C. Y., Epps, J., Lewis, J. W., Szundi, I., Bhagat, A., Sakmar, T. P., and Kliger, D. S. (2007) Photointermediates of the rhodopsin S186A mutant as a probe of the hydrogen-bond network in the chromophore pocket and the mechanism of counterion switch. *J. Phys. Chem. C 111*, 8843–8848.
25. Ahuja, S., Hornak, V., Yan, E. C. Y., Syrett, N., Goncalves, J. A., Hirshfeld, A., Ziliox, M., Sakmar, T. P., Sheves, M., Reeves, P. J., Smith, S. O., and Eilers, M. (2009) Helix movement is coupled to displacement of the second extracellular loop in rhodopsin activation. *Nat. Struct. Mol. Biol. 16*, 168–175.
26. Lewis, J. W., Szundi, I., Kazmi, M. A., Sakmar, T. P., and Kliger, D. S. (2004) Time-resolved photointermediate changes in rhodopsin glutamic acid 181mutants. *Biochemistry 43*, 12614–12621.
27. Thomas, Y. G., Szundi, I., Lewis, J. W., and Kliger, D. S. (2009) Microsecond time-resolved circular dichroism of rhodopsin photointermediates. *Biochemistry 48*, 12283–12289.